

Self-Assembly of a Hexagonal Boron Nitride Nanomesh on Ru(0001)

Andrii Goriachko, Yunbin He, Marcus Knapp, and Herbert Over*

Department of Physical Chemistry, Justus-Liebig-University, Heinrich-Buff-Ring 58,
D-35392 Giessen, Germany

Martina Corso, Thomas Brugger, Simon Berner, Juerg Osterwalder, and Thomas Greber*

Physics Institute, University of Zürich, Winterthurerstrasse 190, CH-8057 Zürich, Switzerland

Received October 11, 2006. In Final Form: December 24, 2006

Hexagonal boron nitride (h-BN) nanostructures were grown on Ru(0001), and are very similar to those previously reported on Rh(111). They show a highly regular 12×12 superstructure, comprising 2 nm wide apertures with a depth of about 0.1 nm. Valence band photoemission reveals two distinctly bonded h-BN species, and X-ray photoelectron spectroscopy indicates an h-BN monolayer film. The functionality of the h-BN/Ru(0001) nanomesh is demonstrated by using this structure for the assembly of gold nanoclusters.

The hexagonal boron nitride (h-BN) nanomesh is an atomically thin, highly regular, and stable nanostructure, first reported for rhodium (111).¹ It grows in a chemical vapor deposition (CVD) process, where borazine (HBNH)₃ vapor leads to the self-assembly of h-BN films on transition metal surfaces at 1000 K. On Rh(111), the nanomesh is a nanostructure with a surface periodicity of about 12×12 substrate unit cells, which corresponds to a lattice constant of 3.2 nm. This periodicity is that of a coincidence lattice given by the misfit between Rh(111) and h-BN (0.27 nm versus 0.25 nm). Interestingly, the h-BN nanomesh reveals 2 nm wide holes or apertures, which makes this nanomesh a promising template with nanopores for a periodic arrangement of molecules or nanometer-sized clusters. In order to understand the self-assembly process of this peculiar h-BN structure and eventually to tailor its apertures and/or lattice constant, one would like to grow nanomeshes on other transition metal substrates as well. However, so far, on other late transition metal surfaces such as palladium (111), no nanomesh was found.² Therefore, it has not been clear whether Rh(111) is unique in the formation of the h-BN nanomesh.

CVD-grown h-BN films on Ru(0001) have already been investigated by low-energy electron diffraction (LEED) and Auger electron spectroscopy (AES).³ The observed 12×12 superstructure was interpreted in terms of a single layer coincidence lattice with 13×13 h-BN units. However, the Ru(0001) surface has an in-plane lattice constant similar to that of Rh(111) (0.271 nm versus 0.270 nm) and similar catalytic activities with respect to the decomposition of borazine (HBNH)₃. This leads to the prediction of similar BN film growth properties and structures of h-BN on Rh(111) and Ru(0001) surfaces. Indeed, the present study, which also comprises a scanning tunneling microscopy (STM) investigation, emphasizes a very similar h-BN nanomesh structure of h-BN/Rh(111) and h-BN/Ru(0001). In extensive X-ray photoelectron spectroscopy (XPS) studies, the h-BN coverages on Rh(111) and Ru(0001) were found to be close to

those reported by Paffet et al.,³ that is, close to a single h-BN sheet on Ru and Rh. Therefore, we also discuss here possible alternatives for the atomic model of the BN nanomesh on rhodium and ruthenium.

We have used a CVD technique to grow h-BN on Ru(0001) identical to that originally applied to Rh(111),¹ utilizing high-purity borazine (HBNH)₃ synthesized by Müller and co-workers.⁴ The decomposition of borazine at 1100 K on transition metal surfaces supplies boron and nitrogen onto the metallic substrate, leading to the self-limiting growth of h-BN.^{2,3,5–7} Figure 1a depicts a LEED pattern of h-BN/Ru(0001) taken at 150 K. The observed pattern is in line with the (12×12) coincidence lattice reported by Paffet et al.,³ indicating a structure with 3.25 nm periodicity. One can discern the first-order spots of the Ru(0001) substrate (arrow-marked as Ru in Figure 1a) and numerous higher-order superstructure spots from the BN nanomesh. The distance between neighboring superstructure spots is related to the nanomesh periodicity in real space. The strongest superstructure spot (arrow-marked as N–N) is related to the distance between neighboring N atoms in the h-BN basal plane, that is, 0.25 nm.

In Figure 1b, we show an STM image of a representative region on the Ru(0001) surface after the h-BN preparation described above. The h-BN nanomesh completely covers the Ru(0001) surface, as checked by an O₂ adsorption experiment. Within the sensitivity of AES, no oxygen can adsorb on the h-BN/Ru(0001) surface.⁸ One finds a structure that strongly resembles the h-BN/Rh(111) nanomesh¹ with dark apertures arranged in a hexagonal lattice and connecting bright wires. Besides this, there are other distinct features in the STM image, numbered as (1) single-layer step edges, (2) double-layer step edges, (3) dark pits, which are deeper than typical nanomesh apertures, (4) subsurface argon bubbles in the form of protrusions of round shape originating from the Ar⁺ sputtering,⁹ and (5) BN-nanomesh domain boundaries. In comparison to h-BN/Rh-

* Corresponding author. Fax.: +49-641-9934559; e-mail: Herbert.Over@phys.chemie.uni-giessen.de (H.O.). Fax.: +41-44-6355704; e-mail: greber@physik.unizh.ch (T.G.).

(1) Corso, M.; Auwärter, W.; Muntwiler, M.; Tamai, A.; Greber, T.; Osterwalder, J. *Science* **2004**, *303*, 217.

(2) Morscher, M.; Corso, M.; Greber, T.; Osterwalder, J. *Surf. Sci.* **2006**, *600*, 3280.

(3) Paffet, M. T.; Simonson, R. J.; Papin, P.; Paine, R. T. *Surf. Sci.* **1990**, *232*, 286.

(4) Müller, F.; Stöwe, K.; Sachdev, H. *Chem. Mater.* **2005**, *17*, 3464.

(5) Nagashima, A.; Tejima, N.; Gamou, Y.; Kawai, T.; Oshima, C. *Phys. Rev. Lett.* **1995**, *75*, 3918.

(6) Preobrajzanski, A.; Vinogradov, A.; Martensson, N. *Surf. Sci.* **2005**, *582*, 21.

(7) Auwärter, W.; Muntwiler, M.; Osterwalder, J.; Greber, T. *Surf. Sci.* **2003**, *545*, L735.

(8) A detailed account of the h-BN/Ru(0001) interaction with O₂ will be given in a separate paper by Goriachko et al.

(9) Gsell, M.; Jakob, P.; Menzel, D. *Science* **1998**, *280*, 717.

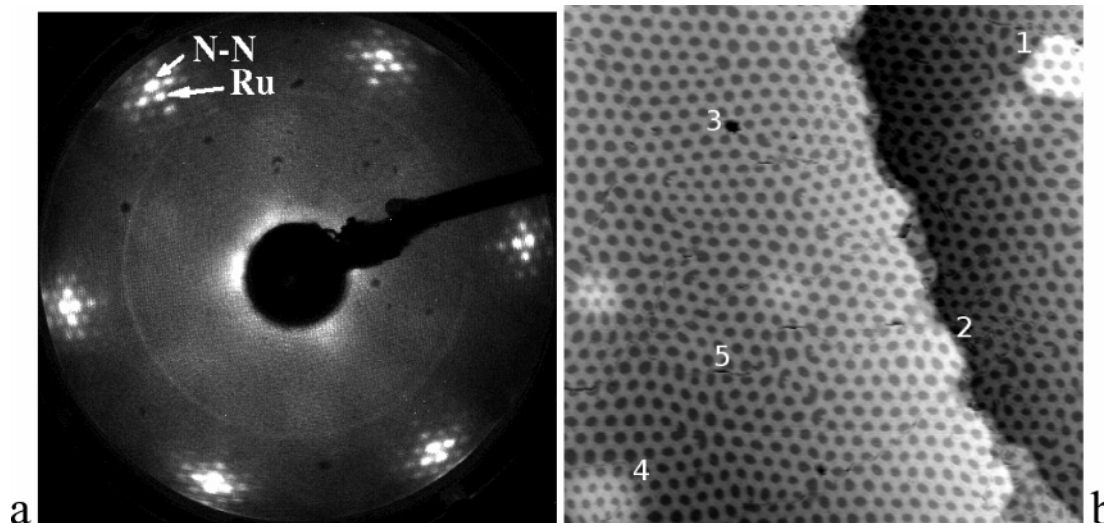


Figure 1. (a) (12×12) LEED pattern from h-BN/Ru(0001) at 90 eV electron energy obtained at a sample temperature of 150 K. The substrate spot (Ru) and the strongest spot of the h-BN nanomesh (N–N) are indicated. (b) STM image of an h-BN nanomesh on Ru(0001): scan size $86 \times 86 \text{ nm}^2$, sample voltage $U_{\text{sample}} = 1.3 \text{ V}$, tunneling current $I_T = 1 \text{ nA}$. The numbers are tags for peculiar features of the h-BN nanomesh: (1) single-layer step edges, (2) double-layer step edges, (3) dark pits, which are deeper than typical nanomesh apertures, (4) subsurface argon bubbles in the form of protrusions of round shape originating from the Ar^+ sputtering, and (5) BN-nanomesh domain boundaries.

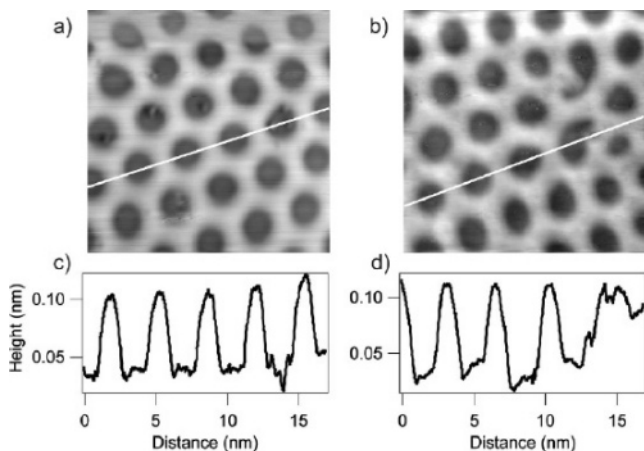


Figure 2. (a,b) Constant-current STM images (-2 V and 1 nA , $13 \times 13 \text{ nm}^2$) of the h-BN nanomeshes on Rh(111) and Ru(0001), respectively. (c,d) Cross-sectional profiles along the white lines in images a and b. The two structures are very similar under the same tunneling conditions. They reveal the same apparent buckling of $0.07 \pm 0.02 \text{ nm}$ between the apertures and the wires, and the same aperture size (2 nm) and wire thickness (1 nm).

(111),¹ the nanomesh shown in Figure 1b is less perfectly ordered. The hexagonal lattice of apertures has frequent distortions that lead to deviations from the mesh periodicity. In contrast to Rh(111), the nanomesh on Ru(0001) does not overgrow the step edges. Rather, we observe an out-of-registry of the periodic arrangement of the apertures when crossing the step edge. The reason for this behavior is seen in the 60° rotation of the surface unit cell of neighboring terraces on hexagonal close-packed (hcp) Ru(0001), while, for the case of face-centered cubic (fcc) Rh(111), such a rotation of the surface unit cell does not occur.

Figure 2 shows two STM images: one from h-BN/Rh(111) and one from h-BN/Ru(0001). For similar tunneling conditions, the two h-BN structures on Ru(0001) and Rh(111) appear very much alike: they have the same aperture size (2 nm) and mesh wire size (1 nm). The cross-sectional profiles shown in Figure 2c,d indicate for both substrates mesh apertures with bottoms that lie about 0.07 nm below the mesh wires. The height modulations of the aperture rims, which cause a 3-fold symmetry,

are much less pronounced (less than 0.02 nm). The specific contribution of different densities of states, tunneling barriers, and true topographic height differences to the observed by STM topography is not clear. Therefore, the above STM data do not allow an unambiguous statement about the true topographic depth of the apertures. In the images of Figure 2, the aperture areas occupy about 30% of the unit cell for Ru and Rh. This value for the aperture area, however, strongly depends on the tunneling conditions, and values of up to 60% were found.

In order to address the question of BN bonding, stoichiometry, and coverage, we performed extensive XPS measurements on h-BN/Ni(111), h-BN/Rh(111), and h-BN/Ru(0001). Figure 3a summarizes normal emission XPS spectra from h-BN/Ru(0001). The measured N1s and B1s binding energies of 389.63 ± 0.15 and $190.83 \pm 0.15 \text{ eV}$, respectively, are typical for h-BN on transition metal surfaces.⁵ In comparison to h-BN/Ni(111), the nitrogen and boron 1s peaks of h-BN/Rh(111) and h-BN/Ru(0001) are broader, indicating differently bonded h-BN species. The coverages for h-BN/Ni(111), h-BN/Rh(111), and h-BN/Ru(0001) turned out to be 1.0 ± 0.25 monolayers and are thus compatible with a single monolayer of stoichiometric h-BN with a lattice constant of 0.25 nm. The error bar is two standard deviations and is mainly caused by the reproducibility of different preparations, where preparations on Rh show the largest scatter. In comparison to the work of Corso et al.,¹ the present coverage determination also takes into account the different surface densities of h-BN and the substrates.¹⁰ It has to be noted that the fcc and the hcp substrate structures have distinctly different normal emission intensities, which are caused by the strong forward scattering peak in the case of hcp structures. This effect was considered in normalizing the Ru emission by an experimentally determined factor of 1.33. In order to minimize systematic errors in the coverage determination, we crosschecked the relative boron coverages of h-BN/Ni(111), h-BN/Rh(111), and h-BN/Ru(0001). The measured B1s intensities on the three samples are identical within a 10% margin, thus supporting the above coverage estimation. The coverage for h-BN/Ru(0001) was independently checked with AES, and, in agreement with Paffet et al.,³ a coverage of one ($\pm 10\%$) monolayer of h-BN on Ru(0001) is concluded.

(10) A detailed account for coverage quantification by photoelectron emission will be given in a separate paper by M. Corso et al.

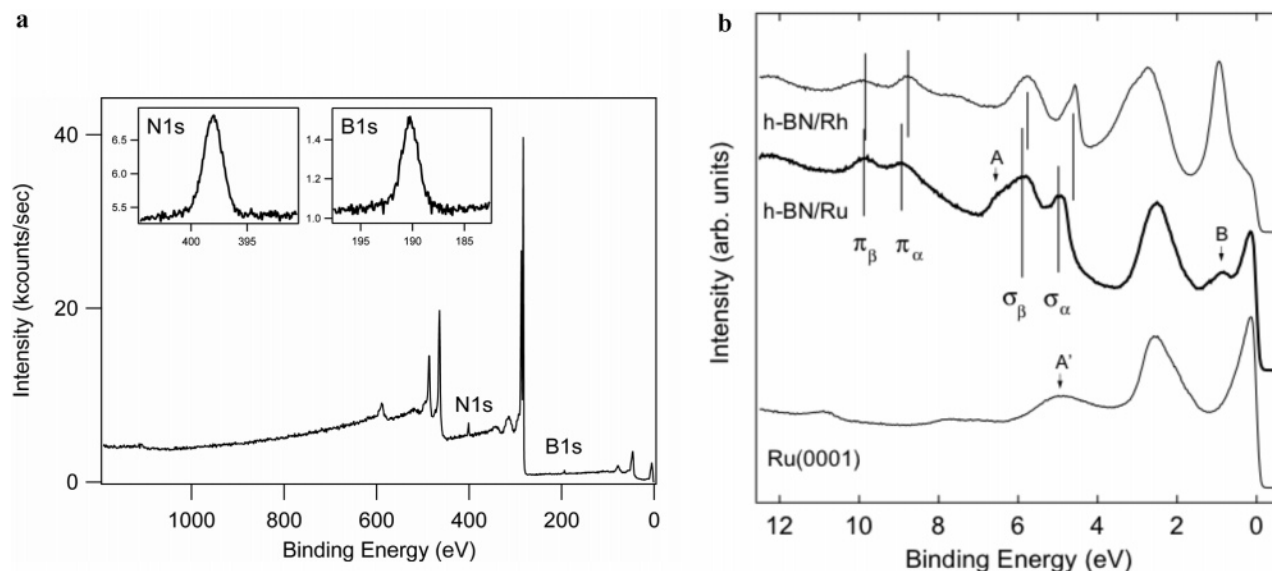


Figure 3. (a) XPS spectrum of h-BN/Ru(0001) measured with monochromatized Al K α radiation. The inset shows the B1s and N1s emissions in more detail. (b) Normal emission UPS spectra of h-BN/Ru(0001), h-BN/Rh(111), and Ru(0001) obtained with He I α 21.2 eV excitation. The h-BN-related features σ_α , σ_β , π_α , and π_β were found to be very similar for h-BN/Ru(0001) and h-BN/Rh(111). The features A and B are assigned to Ru interface states.

Table 1. Experimental Values (in eV) for the Work Function of the Clean and BN-Covered Surfaces, and the Binding Energies for the Two σ and π Bands Measured at the Γ Point with Respect to the Fermi Level

	$\Phi_{\text{substrate}}$	$\Phi_{\text{h-BN}}$	σ_α	σ_β	π_α	π_β
Ru(0001)	5.44 ± 0.10	4.0 ± 0.10	4.97 ± 0.08	5.91 ± 0.15	9.00 ± 0.08	9.83 ± 0.10
Rh(111)	5.50 ± 0.10	4.15 ± 0.10	4.57 ± 0.10	5.70 ± 0.10	8.76 ± 0.08	9.83 ± 0.10

If we compare the valence bands of h-BN/Rh(111) and h-BN/Ru(0001), both systems clearly indicate the “double-layer character”¹ of the BN nanomesh in the electronic structure. This is seen in ultraviolet photoelectron spectroscopy (UPS) and is supported by the XPS core level line widths. A single layer of basal h-BN has four occupied valence bands, that is, three sp^2 -derived σ bands and one p_z -derived π band. Along Γ (i.e., perpendicular to the sp^2 plane), the two low binding σ bands are degenerate and have a lower binding energy than the π band.^{11,12} Figure 3b shows normal emission UPS spectra excited by He I α 21.2 eV radiation for h-BN/Ru(0001), pure Ru(0001), and h-BN/Rh(111). Both BN structures show two σ and two π peaks, albeit at slightly different binding energies with respect to the Fermi level (see Table 1). The σ and π assignment is unambiguously made by measurements of the angular dispersion of the bands (not shown). The lowest lying σ band is not observed since it lies below the ionization threshold of He I α radiation.¹¹ For the case of Ru, we also mark spectral features A, A', and B, which we assign to Ru-related features that change in going from the Ru/vacuum to the h-BN/Ru interface. Up to systematic energy shifts, the electronic structures of h-BN on Ru and Rh are virtually identical. The relative energy shifts may be related to the different work functions and to the slightly different bond strength of h-BN to Ru or Rh. The σ_α peaks show vacuum alignment; that is, adding the work function (see Table 1) to the binding energies yields values of 9.0 and 8.7 eV, respectively. These values correspond within 200 meV to those found by Nagashima et al.⁵ for h-BN/Ni(111), h-BN/Pd(111), and h-BN/Pt(111) σ bands. The alignment to the vacuum level is a consequence of negligible σ hybridization or state mixing with the substrate and the similar charge distribution at the h-BN/vacuum interface.⁵ The high

binding energy σ peaks, σ_β , were assigned to h-BN, which is in direct contact with the metal substrate.¹ The stronger interaction between nitrogen and Ru, Rh compared to that of Ni, and Pd and Pt may contribute to this 1 eV down-shift in binding energy of the σ_β bands, compared to that of the σ_α bands. The σ_β peaks have a weight of 0.69 ± 0.10 and 0.72 ± 0.10 of the overall σ band peak intensities for h-BN/Ru (after subtraction of the interface state A) and h-BN/Rh, respectively. The value for h-BN/Rh(111) is in agreement with the previously reported results.¹

Therefore, intuitively, the binding configurations α and β are related to mesh wires and apertures, respectively, where BN is situated farther or closer away from the substrate. The aperture areas from STM images range from 30 to 60%, and thus this assignment is not straightforward. However, the large range of aperture sizes in STM indicates how sensitively the nanomesh images change under different tunneling conditions. Furthermore, it is not clear how the photoemission cross sections of the σ peaks depend on the registry and height of the BN with respect to the substrate. Given the fact that the apparent aperture width comprises the convolution with the tip shape, the true aperture area should be larger. Therefore, σ_β is assigned to the apertures of the h-BN nanomesh. For the π bands, we find binding energies that follow less strictly the vacuum alignment because of the stronger overlap of the p_z orbitals with substrate orbitals. However, the positions of the π bands agree well with the values observed for h-BN overlayers on various transition metals.^{1,2,5}

We also tested the thermal stability of the h-BN/Ru(0001) nanomesh, which is an important property if the nanomesh is to be used as a template for nanocatalysis, quantum dots, and so forth. On the basis of AES and temperature-programmed desorption (TPD), we conclude that the h-BN/Ru(0001) nanomesh is stable up to 1275 K under ultrahigh vacuum conditions. The Auger spectra of N KLL, Ru MNN, and B KLL are essentially the same before and after annealing to 1275 K for 5 min. The

(11) Catellani, A.; Postermak, N.; Baldereschi, A.; Freeman, A. J. *Phys. Rev. B* **1987**, *36*, 6105.

(12) Grad, G. B.; Blaha, P.; Schwarz, K.; Auwärter, W.; Greber, T. *Phys. Rev. B* **2003**, *68*, 085404.

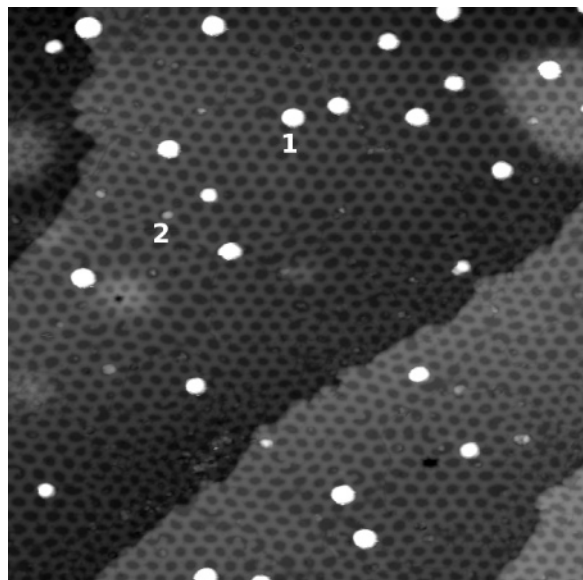


Figure 4. STM image of ~ 0.07 ML of Au deposited on the h-BN/Ru(0001) at room temperature and then annealed to 900 K for 5 min. Numbers indicate large (1) and small (2) particles. The Au nanoparticles are round in shape, and the apparent distortions originate from the nonoptimized STM feedback system reaction.

LEED pattern also showed the same superstructure spots before and after annealing to 1275 K. This means that the BN coverage is preserved after annealing at 1275 K as the nanomesh structure. These results are in line with the TPD experiment, where BN-related species were detected only above a substrate temperature of 1300 K.

Finally, we demonstrate the nanomesh functionality as a template, by evaporating 0.07 ML of Au onto the h-BN/Ru(0001) at room temperature, followed by annealing at 900 K for 5 min. This procedure led to the formation of well-defined round Au nanoparticles on h-BN/Ru(0001) (see Figure 4). Upon annealing, the Au coverage has decreased to ~ 0.05 ML. All Au particles are centered at the nanomesh apertures, and no Au particle is found to be located on the wires. Therefore, the h-BN/Ru(0001) nanomesh indeed acts as a template for the Au particles. We observe two major types of nanoparticles, namely, those larger and smaller than single nanomesh apertures, tagged 1 and 2, respectively, in Figure 4. Larger particles (1) are 4 ± 0.5 nm in diameter and up to 1 nm in height, thus representing partial hemispheres. The small particles (2) precisely fit into apertures; these particles are 1 ± 0.4 nm in diameter.

To outline the present status of the search for alternative nanomesh supporting substrate, we have to tackle the key questions concerning the driving force for nanostructuring of the h-BN film on such substrates as Rh(111) and Ru(0001). Both substrates have a large, but similar lattice mismatch of approximately -7% with respect to the h-BN basal plane, and a relatively strong nitrogen bonding to the metal surface that we believe to be the major reason for the deviation from a simple flat film as encountered on h-BN/Ni(111)⁷ or h-BN/Pd(111).² The bulk values of the in-plane lattice constants of h-BN(0001) and Ru(0001) are 0.25 and 0.271 nm, respectively, suggesting a coincidence lattice with a period of about 12 Ru or 13 h-BN

unit cells. This coincidence lattice is in line with previous experiments.³ The observed structure cannot, however, be explained with a simple coincidence lattice³ or Moiré pattern, as was recently identified with h-BN/Pd(111), where a (10×10) superstructure and a single-layer BN character was observed,² or with graphite on Ru(0001) showing a (11×11) superstructure.¹³ As on h-BN/Rh(111), the electronic structure of h-BN/Ru(0001) shows two distinctly bonded h-BN species, which are likely to be responsible for the functionality as a template with 2 nm apertures (cf. the STM images in Figures 2 and 4). The observed BN coverage is compatible with a single layer of basal h-BN. This BN coverage, together with the difficulty to explain the low apparent aperture depth of 0.07 nm in STM in comparison with the layer distance in bulk h-BN of 0.3 nm, calls for a refined model beyond the previously suggested two-mesh-layer model.¹ The single-layer h-BN model could be a kind of dislocation network structure, with a nonrigid h-BN lattice or, alternatively, a modulated single h-BN basal plane. In any case, the mesh apertures are associated with h-BN regions in close contact with the substrate, presumably being (nearly) on top of nitrogen bonding sites.^{7,12,14} The mesh wires are regions with a loose contact of h-BN with the substrate. Ab initio total energy and electronic structure calculations will help to distinguish between the double- and single-layer model. However, the ultimate determination of the atomic structure of the h-BN nanomesh on Ru(0001) and Rh(111) requires a full surface X-ray diffraction analysis. For the sake of completeness, it is worth mentioning other self-organized nanostructures on the Ru(0001) substrate. A monolayer of Ag forms a superstructure of vacancy islands filled with sulfur, having a typical nanomesh look in STM and a period of 5.3 nm.¹⁵ Finally, sulfur wires just one atom in width form a mesh of hexagons and triangles on a two-monolayer Cu film adsorbed on Ru(0001).¹⁶

In conclusion, we have demonstrated that an h-BN nanomesh can be grown on Ru(0001) by the same recipe used for Rh(111), that is, exposure of about 60 L of borazine at a 1100 K sample temperature. Both nanomeshes are strikingly similar in many aspects, such as a periodicity of 12 substrate unit cells, aperture structures (2 nm wide), and two distinctly bonded h-BN species. For Rh and Ru, we find h-BN coverages that were consistent with a single sheet of h-BN. In the case of h-BN/Ru, the functionality of the nanomesh has been demonstrated by using this structure for the assembly of gold nanoclusters.

Acknowledgment. Enlightening discussions with Peter Blaha and technical support from Martin Klöckner are gratefully acknowledged. Ultrapure borazine was kindly provided by Hermann Sachdev. We gratefully acknowledge the financial support from the European Union under Contract No. NMP4-CT-2004-013817 (NanoMesh).

LA062990T

(13) Wu, M.-C.; Xu, Q.; Goodman, D. W. *J. Phys. Chem.* **1994**, *98*, 5104.
 (14) (a) Gamou, Y.; Terai, M.; Nagashima, A.; Oshima, C. *Science Reports of the Research Institutes, Tohoku University*; Series A: Physics, Chemistry, and Metallurgy; Tohoku University: Sendai, Japan, 1997; p 211. (b) Rokuta, E.; Hasegawa, Y.; Suzuki, K.; Gamou, Y.; Oshima, C.; Nagashima, A. *Phys. Rev. Lett.* **1997**, *79*, 4609.

(15) Pohl, K.; de la Figuera, J.; Bartelt, M. C.; Bartelt, N. C.; Hrbek, J.; Hwang, R. Q. *Surf. Sci.* **1999**, *433–435*, 506.

(16) Hrbek, J.; de la Figuera, J.; Pohl, K.; Jirsak, T.; Rodriguez, J. A.; Schmid, A. K.; Bartelt, N. C.; Hwang, R. Q. *J. Phys. Chem. B* **1999**, *103*, 10557.